ORIGINAL PAPER

DSC Determination of Glass Transition Temperature on Sea Bass (*Dicentrarchus labrax*) Muscle: Effect of High-Pressure Processing

Valeria Tironi · Marie de Lamballerie-Anton · Alain Le-Bail

Abstract Differential scanning calorimetric determination of glass transition temperature in the freeze-concentrated matrix (T_g') of sea bass muscle was optimized. Conventional and modulated differential scanning calorimetry (DSC) techniques (using diverse cooling/heating rate and modulation parameters) and effect of an annealing step (−30, −20, or −15°C, 30min) were assayed. Transition was more evident using conventional DSC assays, cooling/heating rate: 10°C/min, annealing step at –20°C. A T_g' value of –15.2 ± 0.3°C was observed for sea bass fresh muscle. This method was chosen for T_g' determination on high-pressure (HP) treated and pressure shift freezing (PSF)—stored at –20°C—sea bass muscle. Thus, in both cases, transition at –15°C was less evident as a function of the pressure level applied, being very difficult to detect after treatment at 400 and 600MPa. It was observed that T_g' values were shifted to slightly higher temperatures (around 1°C higher) after HP treatment at 400 and 600MPa. The present work constituted a first approach to the study on the effect of HP on the glass transition of a complex food matrix, giving useful information about stability of the frozen food.

Keywords Glass transition · Differential scanning calorimetry · High pressure · Pressure shift-freezing · Fish

Introduction

Glass transition is a second-order thermodynamic transition that has an important impact on food stability. The glass transition corresponds to drastic changes in molecular mobility resulting in possible changes in texture or other physical parameters linked to chemical reactions (Hashimoto et al. 2004). The rate of deterioration is significantly reduced when systems are stored below the glass transition temperature. This is due to the compounds involved in these reactions, which are made less available to feed the reactions over molecular distances due to the reduced diffusion rate (Slade and Levine 1991; Rahman et al. 2003; Hashimoto et al. 2004). When a food system is cooled below its initial freezing temperature, ice formation results in concentration of solutes in the unfrozen phase which become increasingly supersaturated as the cooling is continued, increasing exponentially its viscosity and converting the remaining concentrated aqueous phase from a rubbery unfrozen (unstable and reactive) to a glassy phase (Brake and Fennema 1999). This conversion occurs at the glass transition temperature T_g—more properly a range of temperature—characteristic of the solute involved in the formation of the glassy matrix.

From the point of view of the food stability during frozen storage, glass transition temperature obtained under conditions of maximal freeze concentration (T_g') is the more significant (Goff 1994). T_g' can be achieved by slow freezing and is influenced by the molecular weight of solutes and to a lesser extent by solute conformation and structure (Brake and Fennema 1999). Very different T_g' values have been determined in diverse muscle tissues: beef, −60°C (Rasmussen 1969), −40°C (Simatos et al. 1975); pork loin, −20°C (Levine and Slade 1989); turkey, −13.5°C; chicken, −16.8°C (Delgado and Sun, 2002).

V. Tironi · M. de Lamballerie-Anton · A. Le-Bail (✉)
Nantes Atlantic Universities-ENITIAA-GEPEA (UMR CNRS 6144), Ecole Nationale d'Ingénieurs des Techniques des Industries Agricoles et Alimentaires,
Rue de la Géraudière,
BP 82 225, F-44322 Nantes Cedex 3, France
e-mail: lebail@enitiaa-nantes.fr

Within fish species reported values are also very varied: cod, −77°C (Nesvadba 1993), −40°C (Simatos and Blond 1993), and –15°C (Levine and Slade 1989); tuna: −68 to −71°C (Inoue and Ishikawa 1997), −74°C (Orlien et al. 2003), −11.5 to −18°C (Levine and Slade 1989). Complex products such as plant or animal tissues can exhibit more than one T_g' (Levine and Slade 1989), and the existence of either a high, a low, or both types of T_g' in fish muscle is a subject of investigation (Orlien et al. 2003). However, due to the dominance of high-molecular-weight components in the muscle tissues, the expected T_g' values would be around –10 ± 5°C such as those that occur on many glass-forming polysaccharides and proteins (Slade and Levine 1995). In addition, differential scanning calorimetry (DSC) method applied in the T_g determination has an important influence on the values. Thus, several authors have demonstrated the necessity of carried out an annealing step (i.e., holding the sample at temperature near the T_g' to achieve the maximal freeze concentration) to obtain an accurate T_g' value (Brake and Fennema 1999; Delgado and Sun 2002; Jensen et al. 2003). Nevertheless, this recommendation may be difficult to apply, as the value of T_g' is not known in advance.

High pressure (HP) technology is of increasing interest in food systems in response to consumer demand for safe, high-quality, nutritious foods, due to mainly the fact that it permits to achieve—under certain conditions—microbial and enzymes inactivation at low or moderate temperatures (Cheftel and Culioli 1997; Ludikhuyze and Hendrickx 2002). Recently, potential of HP treatment for creating new ingredients and products has been demonstrated because of its influence on food components (Michel and Autio 2002). In addition, new possibilities for food processing and preservation using HP at temperatures below 0°C are being studied, such as the pressure shift freezing (PSF), pressure-assisted thawing, and other processes (Denys et al. 2002). Pressure treatments induced modifications in food components. Particularly, in fish and meat products, protein denaturation and aggregation is an important consequence of HP application (Cheftel and Culioli 1997).

Effect of HP treatments on glass transition of food systems has not been investigated. Studies on polymers suggest a change of approximately 22K/100MPa for non-hydrogen bonded systems, while on the hydrogen bonded system sorbitol the change is the 4K/100MPa, suggesting that similar orders of magnitude may be expected for glass transition in proteins (Heremans 2002).

Tacking into account that sea bass (Dicentrarchus labrax L.) is an expensive fish, previous work about HP application on this seafood has been performed (Chéret et al. 2006; Tironi et al. 2007). The aims of the present work were, in first term, to determine T_g' on sea bass muscle by establishing a suitable DSC protocol. Then, the effect of different levels of HP application (200, 400 and 600MPa) and PSF process (200, 400 and 600MPa) on this parameter was evaluated to obtain information about stability of sea bass in the frozen state.

Materials and Methods

Materials

Sea bass (Dicentrarchus labrax L.) fresh fishes were obtained from a local market, slaughtered, cleaned, skinned, and filleted within 24h after death. Fillet samples were stored at 4°C until HP treatment (between 4 and 8h). In the case of nonfreezing samples (treated or not with HP, stored at 4°C), DSC determinations were performed within 48h after sampling.

High-pressure Treatments

Fillet pieces were placed in polyethylene bags and vacuum-packed. HP treatments were carried out in a 3.5-l reactor unit (ACB Pressure Systems, Nantes, France) equipped with temperature and pressure regulator device, according to protocols previously applied on sea bass in our laboratory (Chéret et al. 2006; Tironi et al. 2007):

High-pressure application Pressure was increased at 3MPa/s up to the selected pressure level (200, 400, and 600MPa), kept constant during 10min and then rapidly released (2s). Temperature of the transmitting medium (water) was maintained at 10 ± 3°C during the process.

Pressure shift freezing Samples were placed in the vessel, and the pressure was increased to 200, 400 or 600Mpa at a rate of 3Mpa/s. Temperature of the transmitting medium (ethanol/water 50/50% *v/v*) was maintained at −18°C, and samples were kept 30min under pressure to ensure a full cooling down to −18°C. Pressure was rapidly released (2s) to initiate the nucleation process. In the case of pressure of 600MPa, the flesh was undergoing freezing under pressure (pressure supported freezing) with an expected ice III formation. During depressurization from 600MPa, the samples were undergoing crystal change from ice III to ice I with a change in specific volume of +15%. During depressurization from 400MPa, the sample was either unfrozen in supercooling condition or was frozen with ice I crystallization in the case of "supercooling" condition with ice of type I polymorphism instead of ice of type III or at least was frozen with ice III crystallization (Kowalczyk et al. 2005; Urrutia-Benet et al. 2007). After depressurization, samples were stored at −20°C for completion of the freezing under atmospheric conditions. Indeed, after

pressure release, freezing is partial and does not exceed 30% mass ratio for pure water and is of course less for real food (Zhu et al. 2005).

Differential Scanning Calorimetry

Glass transition was analyzed by a Q100 calorimeter (TA Instruments, New Castle, USA). Enthalpy and temperature calibration was performed using indium, and heat capacity calibration was carried out using sapphire.

Optimization of DSC Conditions Diverse DSC methods were applied on fresh sea bass muscle to find the best conditions for the T_g' detection, using conventional and modulated DSC (Table 1). In all cases, a mass between 15 and 18mg of muscle was placed in a DSC pan, and an empty pan was used as reference. For non-annealed samples, the following general protocol was performed: samples in DSC pans were cooled between 20 and –90°C, held at –90°C for 10min, and heated to 20°C applying or not heat modulation. When a step of annealing was applied, the procedure was the following: samples in DSC pans were cooled between 20 and –90°C, held at –90°C for 5min, heated to the annealing temperature holding by 30min, cooling to –90°C, held for 5min; and heated to 20°C applying or not heat modulation.

High-Pressure-Treated Samples

HP-treated samples were analyzed according to method 13 (Table 1), which was also used for fresh muscle. *PSF* samples were maintained in the frozen state without thawing until the start of the DSC run (the loading of the sample in the DSC pan was performed into a freezing room at –20°C, the DSC pans being maintained at –20°C until the installation into the DSC equipment which was previously equilibrated at –20°C). Mass sample of frozen samples was reduced (between 10 and 13mg) in comparison to the case of fresh muscle due to the difficulty in installing a piece of frozen rigid material in the DSC pan. The following DSC protocol was applied: cooling between −20 and −90°C (10°C/min); held at −90°C for 10min; and heated to 20°C (10°C/min).

In all cases, total heat flow (THF), reversible heat flow (RHF)—in the case of modulated DSC runs—and their corresponding first-derivative curves were analyzed using the Universal V3.7A TA Instruments software. T_g' values were obtained as the midpoint of the transition from the heat flow curves and as the peak maximum from the first derivative curves. Moisture content of each sample was determined by drying at 105°C after each run.

Statistical Analysis

T_g' values were analyzed by means of the analysis of variance (ANOVA) according to the General Linear Model Procedure. Significant differences ($p < 0.05$) were evaluated by the least significant differences (LSD) method, according to the Fisher test. Statistical analysis was performed using a Statgraphics plus version 5.0 software (Statistical Graphics, Princeton NJ, USA).

Results and Discussion

Comparison of DSC Methods on Fresh Sea Bass Muscle

As has been previously mentioned, several authors have informed the appearance of a glass transition at very low

Table 1 DSC protocols applied for T_g' determination on sea bass muscle

| Method number°	Cooling rate (°C/min)	Annealing	Heating rate (°C/min)	DSC type/ mod parameters
1	5	None	5	St DSC
2	5	None	5	MDSC/per: 60 seg, A: 0.796°C
3	5	None	3	MDSC/per: 40 seg, A: 0.32°C
4	5	None	1	MDSC/per: 60 seg, A: 0.159°C
5	5	−30°C, 30 min	5	St DSC
6	5	−30°C, 30 min	5	MDSC/per: 60 seg, A: 0.796°C
7	5	−20°C, 30 min	5	St DSC
8	5	−20°C, 30 min	5	MDSC/per: 60 seg, A: 0.796°C
9	10	None	10	St MDSC
10	10	None	10	MDSC/per: 60 seg, A: 1.592°C
11	10	−30°C, 30 min	10	St DSC
12	10	−30°C, 30 min	10	MDSC/per: 60 seg, A: 1.592°C
13	10	−20°C, 30 min	10	st DSC
14	10	−20°C, 30 min	10	MDSC/per: 60 seg, A: 1.592°C
15	10	−15°C, 30 min	10	St DSC
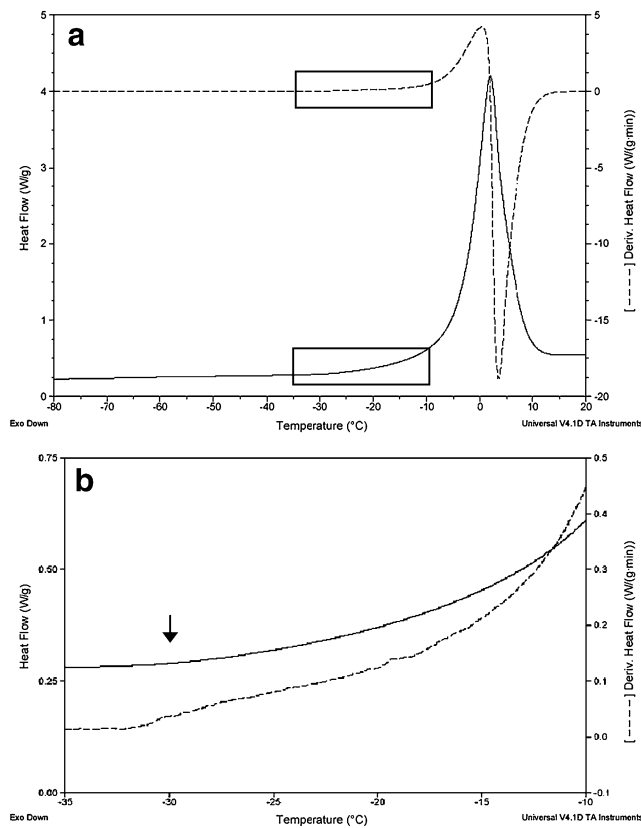
Fig. 1 **a** THF and its first derivative curve obtained on sea bass muscle by conventional DSC (10°C/min—method 9). **b** Enlarged zones showing the heat flow changes. Mass sample: 15.42 mg, moisture: 76.9%

temperatures in muscle systems (between −60 and −80°C; Inoue and Ishikawa 1997; Rasmussen 1969), which has been related to a general phenomenon on protein solutions. However, no transition in this range of temperature could be detected on sea bass, with any of the DSC protocols applied, in agreement with results in cod (Rasmussen 1969). Brake and Fennema (1999) have suggested that this type of transition would not represent a glassy matrix formed by high-molecular-weight components such as the muscle proteins, but a matrix involved low-molecular-weight compounds.

When protocols without an annealing step were performed (methods 1, 2, 3, 4, 9, and 10), a change on the heat flow trace could be detected around −25/−28°C, independently of the cooling and heating rate and the type of DSC run—conventional or modulated—applied. As an example, Fig. 1a shows the THF curve and the first derivative one obtained by conventional DSC with a cooling/heating rate of 10°C/min. The THF change would be related to the beginning of the ice melting and appeared as a light shoulder in the first derivative curve (Fig. 1b).

Modulated differential scanning calorimetry (MDSC) principle is based on the principle that the constant rate of temperature change using conventional DSC is modulated by

superimposing upon it a periodic temperature modulation (generally sinusoidal) of a certain amplitude (A) and frequency or period (per), introducing two different scales of time: a long time scale corresponding to the underlying heating rate and a shorter one corresponding to the period of modulation (Jiang et al. 2002). Thus, it was possible to separate the detected heat flow into two components: the heat capacity-related (reversing) heat flow, and the non-reversing or kinetic heat flow, being the last one caused by processes which are not reversible within the time scale of the period of modulation (Gill et al. 1993; Reading et al. 1994; Orlien et al. 2003). The temperature oscillations were such that the temperature was either constant or was increasing but was never decreasing. This mode called "heat only" was adopted for all MDSC tests. For each heating rate and oscillation period selected, the maximal amplitude recommended by the fabricant to have "heat only" conditions was used. Thermodynamically reversible—within the period of modulation—processes such as glass transition could be observed in the reversing heat flow curves (Orlien et al. 2003). This requires that at least three or five oscillations occur over the span of the researched transition. Conventional vs modulated DSC were compared in the
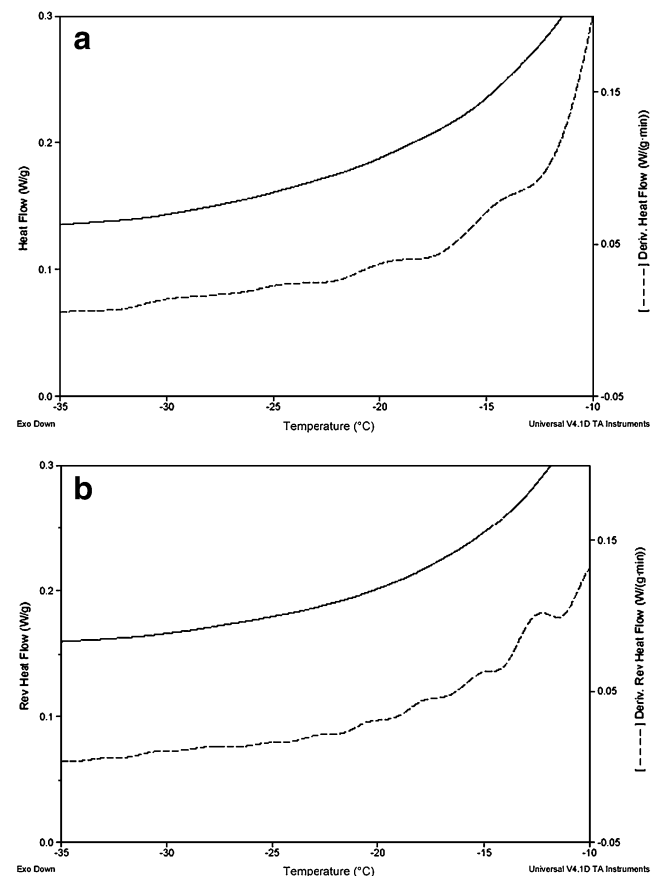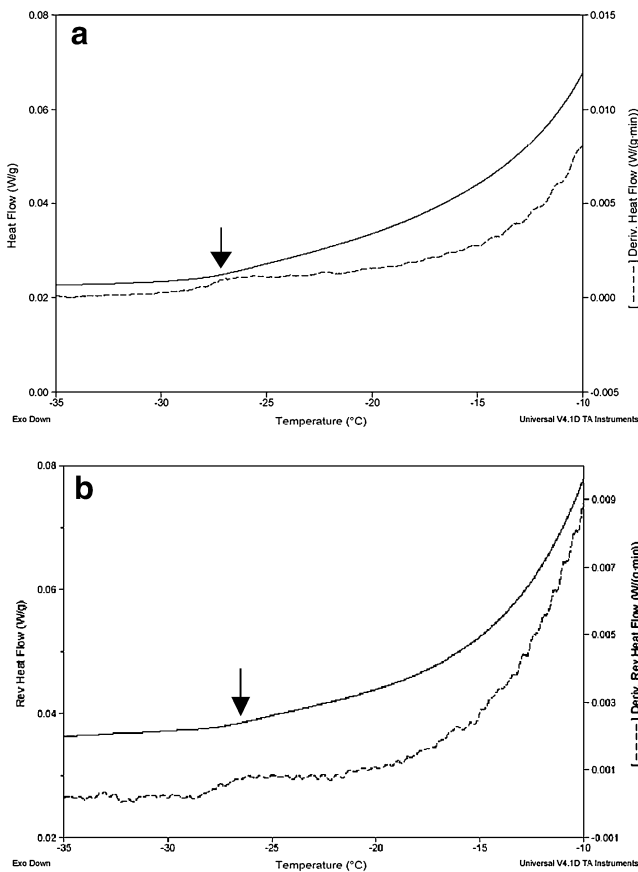

Fig. 2 THF (**a**) and RHF (**b**) and their corresponding first derivative curves obtained on sea bass muscle by MDSC (5°C/min, per: 60 s, **a** 0.796°C—method 2). Mass sample: 16.52 mg, moisture: 78.6%

Fig. 3 THF (**a**) and RHF (**b**) and their corresponding first derivative curves obtained on sea bass muscle by MDSC (1°C/min, per: 60 s, **a** 0.159°C—method 4). Mass sample: 15.03 mg, moisture: 75.3%

present work. DSC curves showed more clear results than MDSC ones using a rate of both 5°C/min (method 1 vs method 2) and 10°C/min (method 9 vs method 10). In MDSC runs (5°C/min, per: 60s, A: 0.796°C), THF curve appear similar to that in the case of conventional runs, while first-derivative THF presented several peaks, which are probably related to the heating rate that is due to the difference (°C) between them which is approximately similar to the rate of heating used (Fig. 2a). This behaviour could be observed also when the cooling/heating rate was 10°C/min (data not shown). As a consequence, it is difficult to extract clear information from MDSC derivative curves with the parameters that we used. RHF curves did not offer additional information, and their derivatives curves appeared very difficult to analyze due to the presence of several small peaks (Fig. 2b).

Different parameters (heating rate, per, A) on MDSC were assayed to improve the determination (methods 2, 3 and 4). A reduced period of the oscillation permits more oscillations over the glass transition. This also leads to a reduced magnitude of the oscillation and in a reduction of the noise to signal ratio. Application of a smaller rate of heating seemed to give better results, because of the multiple

transitions in the derivative heat flow curves. Thus, in this case, it was possible to detect a shift on the baseline of the THF and RHF curves and a peak in the corresponding first-derivative curves that would be associated with a glass transition from both the THF and the RHF curves. Figure 3 shows THF (a) and RHF (b) curves corresponding to heating rate: 1°C/min, per: 60s, A: 0.159°C, presenting a transition value around −26°C. When parameters (heating rate: 3°C/min, per: 40s and A: 0.32°C) were used, results were comparable (data not shown). However, in these cases, transitions were very small, being evident only after analysis of very small-scale values of heat flow. This is in agreement with the theory that the sensitivity decrement as a decreasing heat rate is applied (Zhu et al. 2005).

A transition near −30°C was detected in non-annealing DSC runs. Therefore, an annealing step at this temperature was firstly applied (methods 5, 6, 11, 12) to evaluate if the sample was fully concentrated or not. When samples were maintained during 30min at −30°C, transitions seemed to be more evident, making the detection of glass transition easier in HF and derivative HF curves. In these cases, transition appeared at lower temperatures—between −21 and −23°C—making possible the observation of the beginning of the HF
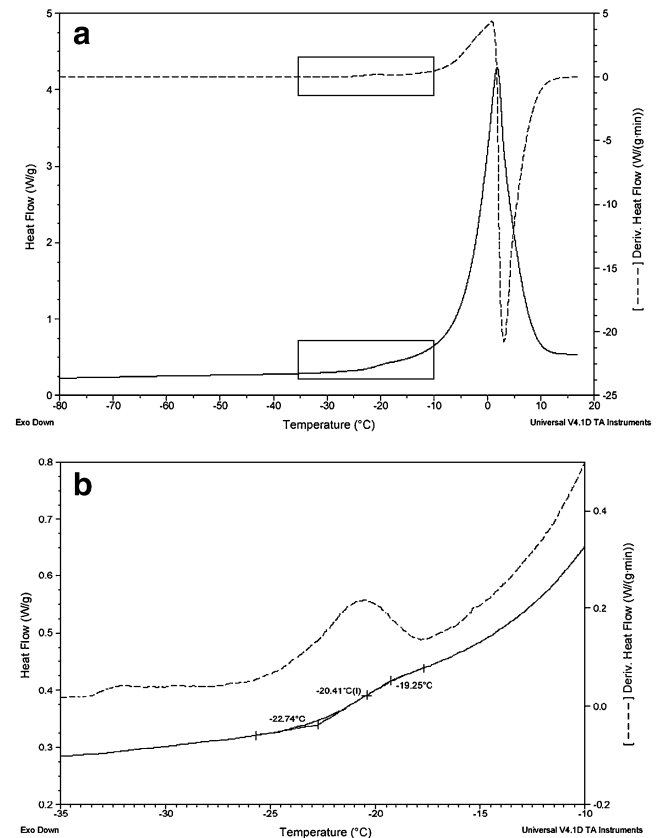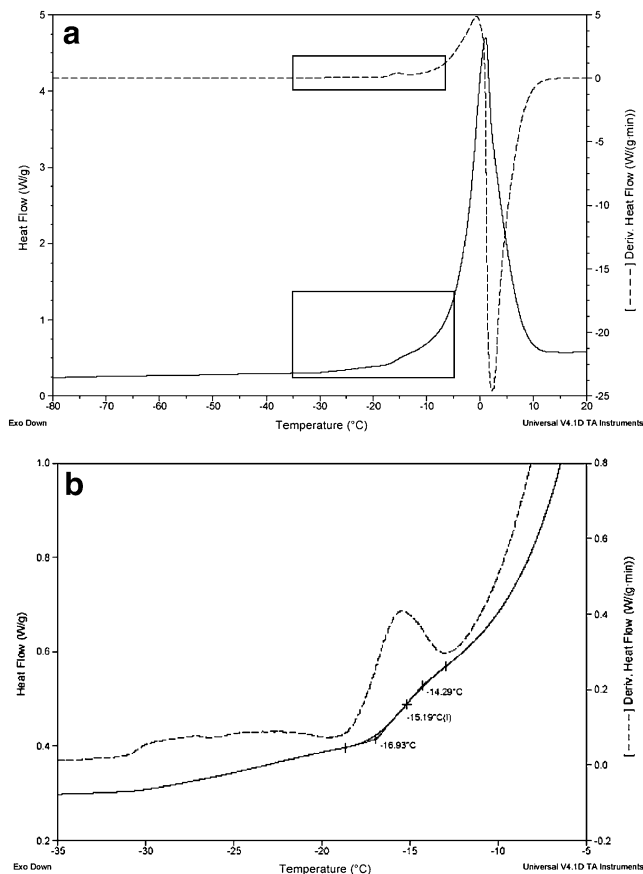

Fig. 4 **a** THF and its first derivative curve obtained on sea bass muscle by conventional DSC applying an annealing step at −30°C, 30 min (10°C/min—method 11). **b** Enlarged zones showing the "glass transition". Mass sample: 15.12 mg, moisture: 76.9%

Fig. 5 a THF and its first derivative curve obtained on sea bass muscle by conventional DSC applying an annealing step at –20°C, 30 min (10° C/min—method 13). b Enlarged zones showing the "glass transition". Mass sample: 16.17 mg, moisture: 76.4%

−33°C in cod muscle, which was interpreted as the beginning of the ice melting. However, when annealing at −30°C, 30min, they detected a glass transition at −21°C (similar result was found in tuna muscle), while if the annealing was at –15°C, 30min, T_g' appeared at −11°C, and if it was at –20°C, 10min, T_g' was -15°C. Meanwhile, Brake and Fennema (1999) obtained the following results in cod muscle: no annealing or annealing at −50°C: no transition; annealing at –20°C, 1h: T_g' = -20°C; annealing at –15°C, 1h: T_g = -12.4°C; annealing at –12°C, 1h: no transition. Results obtained confirm the necessity to optimize the DSC protocol for the T_g' determination and the importance of an annealing step. In the present work, conventional DSC seemed to be more efficient for the determination of T_g' of sea bass muscle. Modulated DSC did not show—in the present matrix and with the assayed parameters—the expected advantages derived from the obtention of the reversible heat flow curves. The conventional DSC (10°C/min) protocol with an annealing step at –20°C, 30min was chosen as the more suitable for the T_g' determination on sea bass muscle. Using this method, a T_g' value of −15.2 ± 0.3°C can be proposed for sea bass muscle, which would be associated with the presence of a glassy matrix formed by the freeze-dehydrated muscle

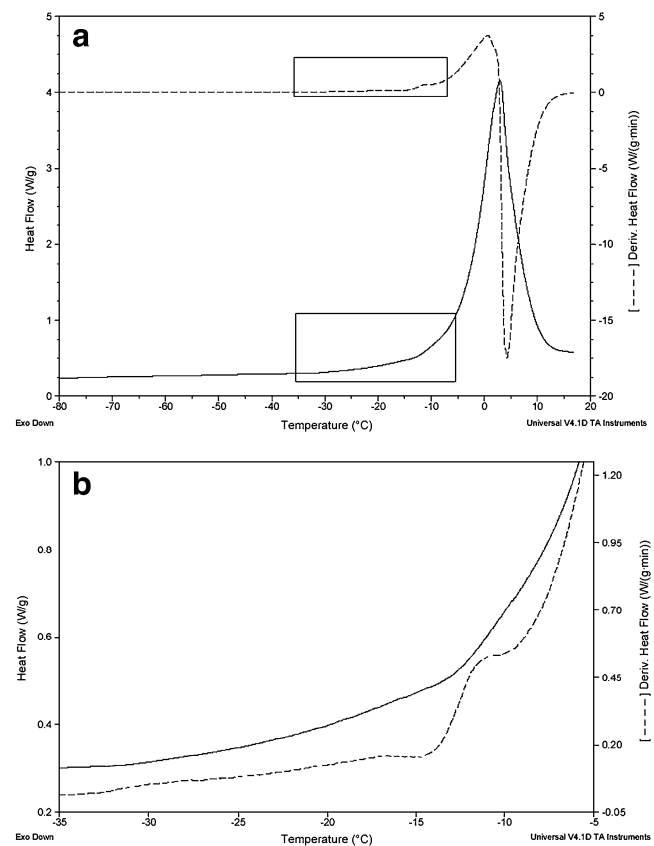increment at around –30°C, as shown in Fig. 4a for conventional DSC (10°C/min). Similarly to non-annealing runs, DSC curves gave more clear results than MDSC ones, obtaining the more evident transition with conventional DSC runs and heating rate of 10°C/min (method 11; Fig. 4b). RHF curves did not give additional or clear information (data not shown).

According to the results obtained with annealing at –30°C, further analysis applying an annealing step at −20°C was performed (methods 7, 8, 13, and 14) to obtain a more accurate value of T_g'. Samples subjected to annealing at −20°C, 30min showed a transition around –15/−16°C (Fig. 5—conventional DSC, 10°C/min). Similarly to the previous assays, conventional DSC gave the more clear results. In accordance to these results, an annealing step at −15°C, 30min, was assayed (method 15). As can be seen in Fig. 6, THF curve did not present an evident glass transition (i.e. a baseline shift), but only an important change of heat flow around −11/−12°C associated with the large endothermic ice-melting peak.

Results can be compared with those informed in other works. Jensen et al. (2003), using conventional DSC (10°C/min), showed a change of the heat flow at around

Fig. 6 a THF and its first derivative curve obtained on sea bass muscle by conventional DSC applying an annealing step at –15°C, 30 min (10° C/min—method 15). b Enlarged zones showing an abrupt change in the heat flow at −12°C. Mass sample: 16.62 mg, moisture: 77.4%

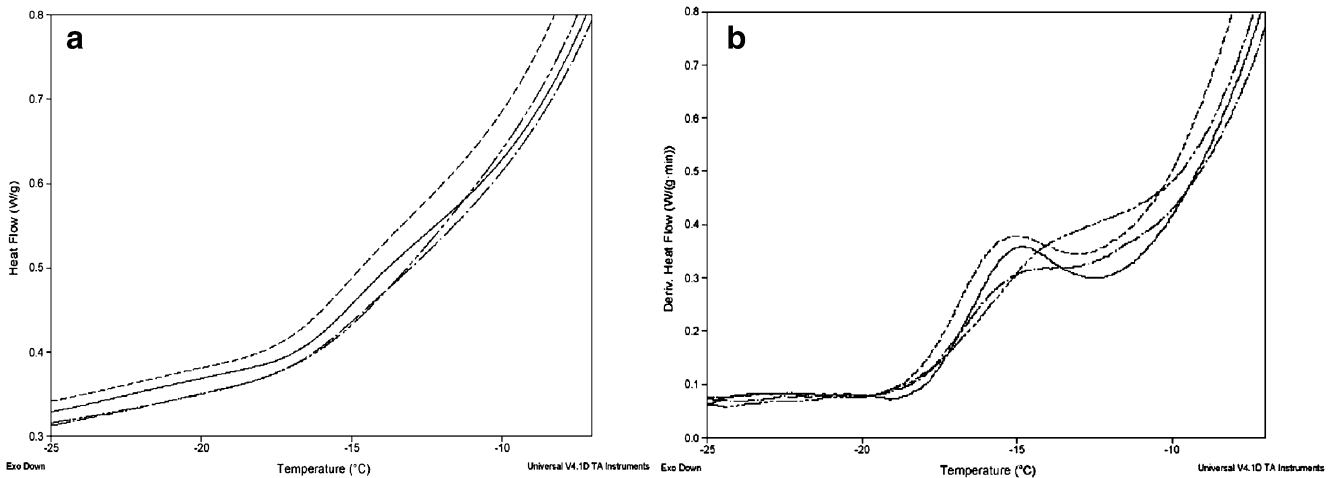Fig. 7 THF (**a**) and its first derivative curve (**b**) obtained by conventional DSC applying an annealing step at −20°C, 30 min (10°C/min—method 13) on HP sea bass muscle: non-pressure treated (mass: 15.72 mg, moisture: 77.9%); 200 MPa, 10 min (mass: 15.81 mg, moisture: 76.1%); 400 MPa, 10 min (mass: 16.29 mg, moisture: 77.7%); 600 MPa, 10 min (mass: 16.29 mg; moisture 76.5%)

proteins. According to this value, a conventional storage at −18°C would be effective to prevent quality deterioration of sea bass muscle, although it is important to take into account the possible temperature variations during the storage that can produce an increase of the temperature product above the T'_g value. However, similarly to other works (Brake and Fennema 1999; Jensen et al. 2003), it is difficult to determine if the detected transition is an effective glass transition or any other transition related to the ice melting and what is its real influence on the storage stability of sea bass.

T'_g determination on HP-treated samples was performed according the selected DSC protocol. An annealing step at −20°C, 30min, was performed on samples pressure treated at room temperature, while on PSF samples, cooling into the DSC equipment starts at −20°C and not the annealing step was carried out during the DSC running due to the storage at –20°C before it. HP-treated samples presented changes in the THF curves as a function of the pressure. Transition at –15°C was less evident as a function of the level of pressure applied (Fig. 7a), being very difficult to detect in the THF curves after 400 and 600MPa (10min) treatment (Fig. 7a), while in derivative curves, the peaks were smaller and with a maximum at higher temperature, especially in the case of 600MPa (Fig. 7b). When the transition temperature was calculated by the software, values showed a progressive shift toward higher temperatures value as the pressure increased, being significantly different after treatment at 400 and 600MPa (Table 2). Comparable results were registered after PSF processes. Glass transition was not evident in THF curves after PSF at
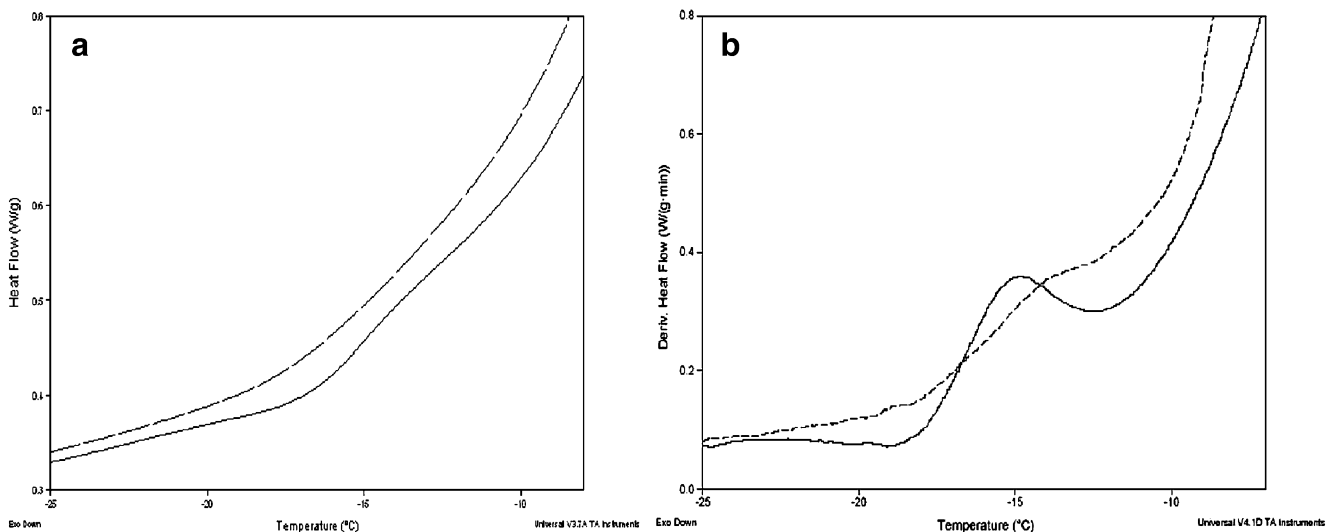

Fig. 8 THF (**a**) and its first derivative curve (**b**) obtained by conventional DSC (10°C/min) on PSF sea bass muscle: non-pressure treated, applying an annealing step at −20°C, 30 min (method 13) (mass: 15.72 mg, moisture: 77.9%); 400 MPa, 10 min, after storage at –20°C (mass: 12.31 mg, moisture: 77.7%)

Table 2 T'_g values of high-pressure treated sea bass muscle

Treatment	Pressure/time (MPa/10 min)	T'_g
None	–	-15.2 ± 0.3^a
HP	200	-14.8 ± 0.1^a
	400	-14.2 ± 0.5^b
	600	-13.9 ± 0.2^b
PSF	200	-14.7 ± 0.2^a
	400	-13.6 ± 0.1^b
	600	-14.1 ± 0.4^b

Each value is represented as mean±SD of at least two determinations. Different letters (a, b) indicate significant differences ($p<0.05$)

400 and 600 MPa (30 min; Fig. 8a) and peaks in derivatives curves appeared very small. Transition temperature values are shown in Table 2.

It is known that pressure treatment causes denaturation and aggregation of fish muscle proteins (Ohshima et al. 1993; Chevalier et al. 2000). Specifically, HP application (200 MPa) during the PSF and the pressure-assisted thawing of sea bass muscle produced a partial denaturation with aggregation and insolubilization of the myosin and other myofibrillar proteins, and alterations of the sarcoplasmic proteins (Tironi et al. 2007). Taking into account the hypothesis that the transition at −15°C can be attributed to a glass transition due to the high molecular weight components of muscle (Brake and Fennema 1999), modifications on the protein structures because of the HP application would be the cause of the changes in this transition. Due to the fact that aggregation produces an increase of the molecular weight of the muscle proteins, an increase of the T'_g value would be expected. An increase of T'_g value by nearly 1°C has been reported by cross-linking of corn starch and of the synthetic polymers (Chung et al. 2004). This change has been explained because the cross-linking reduces the chain mobility in the freeze-concentrated matrix, increasing the glass transition temperature and reducing the change in the specific heat capacity. These observations are comparable to those registered on HP-treated sea bass. So, a possible explanation for the small diminution of the T'_g value (around 1°C) and the decrease on the specific heat capacity (less evident transitions) registered could be related to the protein aggregation process on the HP fish muscle, which would induce a less mobility of the protein chains.

Conclusions

The evaluation of the glass transition temperature in foods remains a difficult objective. The present work confirms the necessity to optimize the DSC protocol for T'_g determination

and the importance of an annealing step. Despite of the expected results according to the theory of MDSC, this technique did not show improvements—in the present matrix and with the assayed parameters—in the T'_g measures. Conventional DSC (10°C/min) with an annealing step at −20°C, 30 min was chosen as more suitable for the T'_g determination on sea bass muscle. Using this method, a T'_g value of –15.2±0.3°C can be proposed for sea bass muscle, which would be associated with the presence of a glassy matrix formed by the freeze-dehydrated muscle proteins.

Mentioned DSC protocol was chosen for T'_g determination on HP and PSF—stored at −20°C—sea bass muscle. In both cases, transition at –15°C was less evident as a function of the pressure level applied (200, 400 and 600 MPa), being very difficult to detect after treatment at 400 and 600 MPa. In addition, T'_g values were shifted to slightly higher temperatures (around 1°C higher) after HP treatment at 400 and 600 MPa. This change would be associated with a change in the conformation and aggregation of the muscle proteins, resulting in higher molecular weight species. The present work is a first approach concerning the study of the influence of the HP treatments on the glass transition; indeed, no other references were found in the existing literature. Further work is thus necessary to better understand the impact of HP and to analyze the real effect of HP treatment on the frozen storage stability of foods.

References

Brake, N., & Fennema, O. (1999). Glass transition values of muscle tissue. *Journal of Food Science, 64*(1), 10–15.

Cheftel, J., & Culioli, J. (1997). Effects of high-pressure on meat: a review. *Meat Science, 46*(3), 211–236.

Chéret, R., Chapleau, N., Delbarre-Ladrat, C., Verrez-Bagnis, V., & de Lamballerie, M. (2006). Effects of high-pressure on texture and microstructure of sea bass (*Dicentrarchus labrax* L.) fillets. *Journal of Food Science, 70*(8), 477–483.

Chevalier, D., Sequeira-Munoz, A., Le Bail, A., Simpson, B., & Ghoul, M. (2000). Effect of pressure shift freezing, air-blast freezing and storage on some biochemical and physical properties of turbot (*Scophthalmus maximus*). *Lebensmittel-Wissenschaft Technologie, 33*, 570–577.

Chung, H., Woo, K., & Lim, S. (2004). Glass transition and enthalpy relaxation of cross-linked corn starches. *Carbohydrate Polymers, 55*, 9–15.

Delgado, A., & Sun, D.–W. (2002). Desorption isotherms and glass transition temperature for chicken meat. *Journal of Food Engineering, 55*, 1–8.

Denys, S., Schlüter, O., Hendrickx, M., & Knorr, D. (2002). Effects of high pressure on water-ice transitions in foods. In Hendrickx, & Knorr (Eds.) *Ultra high-pressure treatments of foods, chapter 8* (pp. 215–248). New York, USA: Kluwer Academic/Plenum Publishers.

Gill, P., Sauerbrunn, S., & Reading, M. (1993). Modulated differential scanning calorimetry. *Journal of Thermal Analysis, 40*, 931–939.

Goff, H. (1994). Measuring and interpreting the glass transition in frozen foods and model systems. *Food Research International, 27*, 187–189.

Hashimoto, T., Suzuki, T., Hagiwara, T., & Takai, R. (2004). Study on the glass transition for several processed fish muscles and its protein fractions using differential scanning calorimetry. *Fisherie Science, 70*, 1144–1152.

Heremans, K. (2002). The effects of high pressure on biomaterials. In Hendrickx, & Knorr (Eds.) *Ultra high pressure treatments of foods, chapter 2* (pp. 23–51). New York, USA: Kluwer Academic/Plenum Publishers.

Inoue, C., & Ishikawa, M. (1997). Glass transition of tuna flesh at low temperature and effects of salts and moisture. *Journal of Food Science, 62*(3), 496–499.

Jensen, K., Jorgensen, B., & Nielsen, J. (2003). Low-temperature transitions in cod and tuna determined by differential scanning calorimetry. *Lebensmittel-Wissenschaft Technologie, 36*, 369–374.

Jiang, Z., Imrie, C., & Hutchinson, J. (2002). An introduction to temperature modulated differential scanning calorimetry (TMDSC): a relatively non-mathematical approach. *Thermochimica Acta, 387*, 75–93.

Kowalczyk, W., Hartmann, C., Luscher, C., Pohl, M., Delgado, A., & Knorr, D. (2005). Determination of thermophysical properties of foods under high hydrostatic pressure in combined experimental and theoretical approach. *Inner Food Science & Emerging Technologies, 6*(3), 318–326.

Levine, H., & Slade, L. (1989). Response to the letter by Simatos, Blond, and Le Meste on the relation between glass transition and stability of a frozen product. *Cryo Letters, 10*, 347–370.

Ludikhuyze, L., & Hendrickx, M. (2002). Effects of high pressure on chemical reactions related to food quality. In Hendrickx, & Knorr (Eds.) *Ultra high-pressure treatments of foods chapter 6*, (pp. 167–188). New York, USA: Kluwer Academic/Plenum Publishers.

Michel, M., & Autio, K. (2002). Effects of high pressure on protein and polysaccharide-based structures. In Hendrickx, & Knorr (Eds.) *Ultra high-pressure treatments of foods chapter 7* (pp. 189–214). New York, USA: Kluwer Academic/Plenum Publishers.

Nesvadba, P. (1993). Glass transition in aqueous solutions and foodstuffs. In Blanshard, & Lillford (Eds.) *The glassy state in foods* (pp. 523–526). Loughborough, UK: Nottingham University Press.

Ohshima, T., Ushio, H., & Koizumi, C. (1993). High-pressure processing of fish and fish products. *Trend in Food Science and Technology, 4*, 370–375.

Orlien, V., Risbo, J., Andersen, M., & Skibsted, L. (2003). The question of high- or low- temperature glass transition in frozen fish. Construction of the supplemented state diagram for tuna muscle by differential scanning calorimetry. *Journal of Agriculture and Food Chemistry, 51*, 211–217.

Rahman, M., Kasapis, S., Guizani, N., & Al-Amri, O. (2003). State diagram of tuna meat: freezing curve and glass transition. *Journal of Food Engineering, 57*, 321–326.

Rasmussen, D. (1969). A note about " phase diagrams" of frozen tissue. *Biodynamical, 10*, 333–339.

Reading, M., Luget, A., & Wilson, R. (1994). Modulated differential scanning calorimetry. *Thermochimica Acta, 238*, 295–307.

Simatos, D., & Blond, G. (1993). Some aspects of the glass transition in frozen foods systems. In Blanshard, & Lillford (Eds.) *The glassy state in foods* (pp. 395–415). Loughborough, UK: Nottingham University Press.

Simatos, D., Faure, M., Bonjour, E., & Couach, M. (1975). Differential thermal analysis and differential scanning calorimetry in the study of water in foods. In Duckwroth (Ed.) *Water relations in foods* (pp. 193–209). London, UK: Academic Press.

Slade, L., & Levine, H. (1991). Beyond water activity: recent advances based on an alternative approach to the assessment of food quality and safety. *Critical Review in Food Science and Nutrition, 30*, 115–360.

Slade, L., & Levine, H. (1995). Water and glass transition—Dependence of the glass transition on composition and chemical structure: special implications for flour functionality in cookie baking. *Journal of Food Engineering, 24*, 431–509.

Tironi, V., de Lamballerie, M., & Le Bail, A. (2007). Effects of pressure shift freezing and pressure assisted thawing on sea bass (*Dicentrarchus labrax*) quality. *Journal of Food Science, 72*(7), 381–387.

Urrutia-Benet, G., Balogh, T., Schneider, J., & Knorr, D. (2007). Metastable phases during high-pressure–low-temperature processing of potatoes and their impact on quality-related parameters. *Journal of Food Engineering, 78*(2), 375–389.

Zhu, S., Ramaswamy, H., & Le-Bail, A. (2005). High-pressure calorimetric evaluation of ice crystal ratio formed by rapid depressurization during pressure-shift freezing of water and pork muscle. *Food Research International, 38*(2), 193–201.